

System size effects in the N/Z dependence of balance energy for isotopic series

Sakshi Gautam^a and Aman D. Sood^{b1}

^a*Department of Physics, Panjab University, Chandigarh -160 014, India.*

^b*SUBATECH, Laboratoire de Physique Subatomique et des Technologies Associées, Université de Nantes - IN2P3/CNRS - EMN 4 rue Alfred Kastler, F-44072 Nantes, France.*

We study the system size effects in the N/Z dependence of balance energy for the isotopic series. We find drastic effect of symmetry energy on the N/Z dependence of E_{bal} throughout the mass range. We also find that the N/Z dependence of E_{bal} for isotopic series of lighter system is slightly more sensitive to symmetry energy as compared to that of heavier systems. We also study the mass dependence of E_{bal} for the N/Z range from 1.0-2.0. We find that the mass dependence of E_{bal} varies with the N/Z ratio.

¹Email: amandsood@gmail.com

1 Introduction

The investigation of the system size effects in various phenomena of heavy-ion collisions has attracted a lot of attention. The system size dependences have been reported in various phenomena like fusion-fission, particle production, multifragmentation, collective flow (of nucleons/fragments) as well as its disappearance, density, temperature and so on [1–15]. For instance, in Ref. [4] the power law scaling ($\propto A^\tau$) of pion/kaon production with the size of the system has been reported. Similar power law behavior for the system size dependence has been reported for the multiplicity of various types of fragments also [5]. The collective transverse in-plane flow has also been investigated extensively during the past three decades and has been found to depend strongly on the combined mass of the system [12] in addition to the incident energy [13, 14] as well as colliding geometry [14]. The energy dependence of collective transverse in-plane flow has led us to its disappearance. The energy at which flow disappears has been termed as the balance energy (E_{bal}) or the energy of vanishing flow (EVF) [15]. E_{bal} has been found to depend strongly on the combined mass of the system [7, 8]. Similarly the power law mass dependences have also been reported for density, temperature, and participant-spectator matter [6].

With the advent of radioactive ion beams [16–18] the role of isospin degree of freedom on dynamics of heavy-ion collisions has been studied for the past decade. These studies are helpful to extract information about the asymmetric nuclear matter. The isospin effects have been explained in literature as the competition among various reaction mechanisms, such as nn collisions, symmetry energy, surface properties and Coulomb force. The relative importance among these reaction mechanisms is not yet clear [19]. Therefore, to explain the relative contribution among these reaction mechanisms, Gautam *et al.* have studied E_{bal} as a function of combined mass of the system [20] as well as colliding geometry for isobaric pairs [21]. There we find that throughout the mass range and colliding geometry, the systems with higher N/Z has larger E_{bal} as compared to the systems with lower N/Z. This was found to be due to the dominance of Coulomb repulsion over symmetry energy in isospin effects throughout the mass range and colliding geometry. Therefore, to take out the role of dominant Coulomb Sod has studied the E_{bal} for a series of isotopes of Ca with N/Z varying from 1.0 to 2.0 [22]. Sood has found that although for an individual isotope E_{bal} is sensitive to symmetry energy as well as its density dependence, isospin-dependent cross section, equation of state (EOS) of symmetric nuclear

matter simultaneously, however the N/Z dependence of E_{bal} showed sensitivity not only to symmetry energy but more importantly to the density dependence of symmetry energy as well. In the present paper, our aim is at least two fold.

- (1) To study N/Z dependence of E_{bal} for isotopic series throughout the mass range and also to explore the effect of symmetry energy.
- (2) To study mass dependence of E_{bal} for various N/Z ratios covering pure symmetric systems to highly neutron-rich ones.

For the present study we use isospin-dependent quantum molecular dynamics (IQMD) model [23].

2 The Model

The IQMD model is an extension of the QMD model [24, 25], which treats different charge states of nucleons, deltas and pions explicitly, as inherited from the Vlasov-Uehling-Uhlenbeck (VUU) model. The IQMD model has been used successfully for the analysis of a large number of observables from low to relativistic energies. The isospin degree of freedom enters into the calculations via symmetry potential, cross sections and Coulomb interaction.

In this model, baryons are represented by Gaussian-shaped density distributions

$$f_i(\vec{r}, \vec{p}, t) = \frac{1}{\pi^2 \hbar^2} \exp(-[\vec{r} - \vec{r}_i(t)]^2 \frac{1}{2L}) \times \exp(-[\vec{p} - \vec{p}_i(t)]^2 \frac{2L}{\hbar^2}) \quad (1)$$

Nucleons are initialized in a sphere with radius $R = 1.12 A^{1/3}$ fm, in accordance with the liquid-drop model. Each nucleon occupies a volume of h^3 , so that phase space is uniformly filled. The initial momenta are randomly chosen between 0 and Fermi momentum (\vec{p}_F). The nucleons of the target and projectile interact by two- and three-body Skyrme forces, Yukawa potential, and Coulomb interactions. In addition to the use of explicit charge states of all baryons and mesons, a symmetry potential between protons and neutrons corresponding to the Bethe-Weizsacker mass formula has been included. The hadrons propagate using the Hamilton equations of motion:

$$\frac{d\vec{r}_i}{dt} = \frac{d\langle H \rangle}{d\vec{p}_i}, \quad \frac{d\vec{p}_i}{dt} = -\frac{d\langle H \rangle}{d\vec{r}_i} \quad (2)$$

with

$$\begin{aligned}
\langle H \rangle &= \langle T \rangle + \langle V \rangle \\
&= \sum_i \frac{p_i^2}{2m_i} + \sum_i \sum_{j>i} \int f_i(\vec{r}, \vec{p}, t) V^{ij}(\vec{r}', \vec{r}) \\
&\quad \times f_j(\vec{r}', \vec{p}', t) d\vec{r} d\vec{r}' d\vec{p} d\vec{p}'.
\end{aligned} \tag{3}$$

The baryon potential V^{ij} , in the above relation, reads as

$$\begin{aligned}
V^{ij}(\vec{r}' - \vec{r}) &= V_{Skymre}^{ij} + V_{Yukawa}^{ij} + V_{Coul}^{ij} + V_{sym}^{ij} \\
&= [t_1 \delta(\vec{r}' - \vec{r}) + t_2 \delta(\vec{r}' - \vec{r}) \rho^{\gamma-1} (\frac{\vec{r}' + \vec{r}}{2})] \\
&\quad + t_3 \frac{\exp(|(\vec{r}' - \vec{r})|/\mu)}{(|(\vec{r}' - \vec{r})|/\mu)} + \frac{Z_i Z_j e^2}{|\vec{r}' - \vec{r}|} \\
&\quad + t_4 \frac{1}{\rho_0} T_{3i} T_{3j} \delta(\vec{r}_i' - \vec{r}_j).
\end{aligned} \tag{4}$$

Here $t_4 = 4C$ with $C = 32$ MeV and Z_i and Z_j denote the charges of the i th and j th baryon, and T_{3i} and T_{3j} are their respective T_3 components (i.e. $1/2$ for protons and $-1/2$ for neutrons). The parameters μ and t_1, \dots, t_4 are adjusted to the real part of the nucleonic optical potential. For the density dependence of the nucleon optical potential, standard Skyrme-type parametrization is employed. We use a soft equation of state along with the standard isospin- and energy-dependent cross section reduced by 20%, i.e. $\sigma = 0.8 \sigma_{nn}^{free}$. For the density dependence of symmetry energy, we use the form $F_1(u) \propto u$ (where $u = \frac{\rho}{\rho_0}$) which is obtained by changing the density dependence of potential part of symmetry energy (last term in equation 4). F_2 represents calculations without symmetry energy. The symmetry energy is switched off by making the potential part of symmetry energy zero. In a recent study, Gautam *et al.* [21] has confronted the theoretical calculations of IQMD with the data of $^{58}Ni + ^{58}Ni$ and $^{58}Fe + ^{58}Fe$ [26]. The results with the soft EOS (along with the momentum-dependent interactions) and above choice of cross section are in good agreement with the data at all colliding geometries. The details about the elastic and inelastic cross sections for proton-proton and proton-neutron collisions can be found in [23, 27]. The cross sections for neutron-neutron collisions are assumed to be equal to the proton-proton cross sections. Two particles collide if their minimum distance d fulfills

$$d \leq d_0 = \sqrt{\frac{\sigma_{tot}}{\pi}}, \sigma_{tot} = \sigma(\sqrt{s}, type), \tag{5}$$

where 'type' denotes the ingoing collision partners (N-N....). Explicit Pauli blocking is also included; i.e. Pauli blocking of the neutrons and protons is treated separately. We

assume that each nucleon occupies a sphere in coordinate and momentum space. This trick yields the same Pauli blocking ratio as an exact calculation of the overlap of the Gaussians will yield. We calculate the fractions P_1 and P_2 of final phase space for each of the two scattering partners that are already occupied by other nucleons with the same isospin as that of scattered ones. The collision is blocked with the probability

$$P_{block} = 1 - [1 - \min(P_1, 1)][1 - \min(P_2, 1)], \quad (6)$$

and, correspondingly is allowed with the probability $1 - P_{block}$. For a nucleus in its ground state, we obtain an averaged blocking probability $\langle P_{block} \rangle = 0.96$. Whenever an attempted collision is blocked, the scattering partners maintain the original momenta prior to scattering.

3 Results and discussions

We simulate the reactions of Ca+Ca, Ni+Ni, Zr+Zr, Sn+Sn, and Xe+Xe with N/Z varying from 1.0 to 2.0 in small steps of 0.2. In particular we simulate the reactions of $^{40}\text{Ca}+^{40}\text{Ca}$ ($N/Z=1$), $^{44}\text{Ca}+^{44}\text{Ca}$ ($N/Z=1.2$), $^{48}\text{Ca}+^{48}\text{Ca}$ ($N/Z=1.4$), $^{52}\text{Ca}+^{52}\text{Ca}$ ($N/Z=1.6$), $^{56}\text{Ca}+^{56}\text{Ca}$ ($N/Z=1.8$), and $^{60}\text{Ca}+^{60}\text{Ca}$ ($N/Z=2.0$); $^{56}\text{Ni}+^{56}\text{Ni}$, $^{62}\text{Ni}+^{62}\text{Ni}$, $^{68}\text{Ni}+^{68}\text{Ni}$, $^{72}\text{Ni}+^{72}\text{Ni}$, and $^{78}\text{Ni}+^{78}\text{Ni}$; $^{81}\text{Zr}+^{81}\text{Zr}$, $^{88}\text{Zr}+^{88}\text{Zr}$, $^{96}\text{Zr}+^{96}\text{Zr}$, $^{104}\text{Zr}+^{104}\text{Zr}$, and $^{110}\text{Zr}+^{110}\text{Zr}$; $^{100}\text{Sn}+^{100}\text{Sn}$, $^{112}\text{Sn}+^{112}\text{Sn}$, $^{120}\text{Sn}+^{120}\text{Sn}$, $^{129}\text{Sn}+^{129}\text{Sn}$, and $^{140}\text{Sn}+^{140}\text{Sn}$; and $^{110}\text{Xe}+^{110}\text{Xe}$, $^{120}\text{Xe}+^{120}\text{Xe}$, $^{129}\text{Xe}+^{129}\text{Xe}$, $^{140}\text{Xe}+^{140}\text{Xe}$, and $^{151}\text{Xe}+^{151}\text{Xe}$ at $b/b_{max} = 0.2 - 0.4$. The reactions are followed till the transverse in-plane flow saturates. It is worth mentioning here that the saturation time varies with the mass of the system. It has been shown in Ref. [11] that the transverse in-plane flow in lighter colliding nuclei saturates earlier compared to heavy colliding nuclei. Saturation time is about 100 (200 fm/c) in lighter (heavy) colliding nuclei in the present energy domain. We use the quantity "directed transverse momentum $\langle p_x^{dir} \rangle$ " to define the nuclear transverse in-plane flow, which is defined as [11, 23, 24, 28]

$$\langle p_x^{dir} \rangle = \frac{1}{A} \sum_{i=1}^A \text{sign}\{y(i)\} p_x(i), \quad (7)$$

where $y(i)$ and $p_x(i)$ are, respectively, the rapidity (calculated in the center of mass system) and the momentum of the i^{th} particle. The rapidity is defined as

$$Y(i) = \frac{1}{2} \ln \frac{\vec{E}(i) + \vec{p}_z(i)}{\vec{E}(i) - \vec{p}_z(i)}, \quad (8)$$

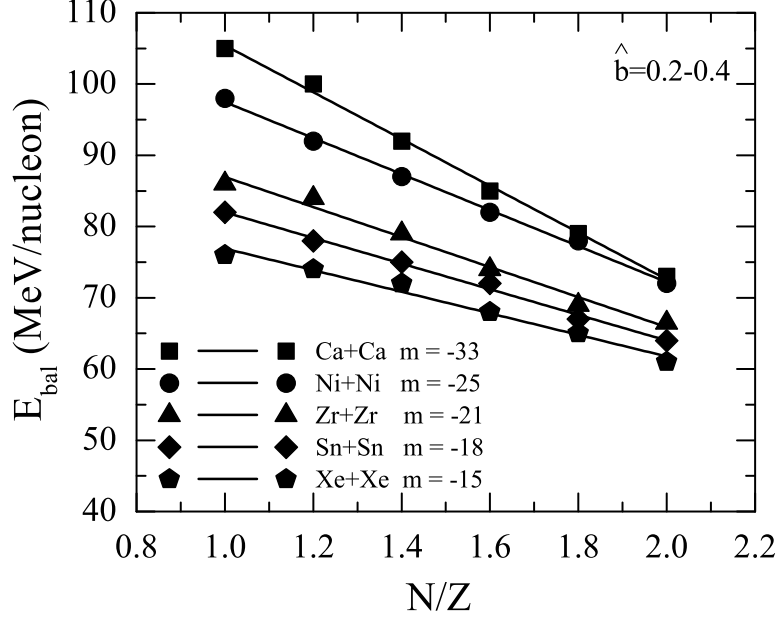


Figure 1: N/Z dependence of E_{bal} for various systems. Various symbols are explained in the text. Lines are linear fit.

where $\vec{E}(i)$ and $\vec{p}_z(i)$ are, respectively, the energy and longitudinal momentum of the i^{th} particle. In this definition, all the rapidity bins are taken into account. It is worth mentioning that the E_{bal} has the same value for all fragments types [26, 29–31]. Further the apparatus corrections and acceptance do not play any role in calculation of the E_{bal} [29, 31, 32].

In Fig. 1, we display N/Z dependence of E_{bal} for isotopes of Ca+Ca (squares), Ni+Ni (circles), Zr+Zr (triangles), Sn+Sn (diamonds), and Xe+Xe (pentagons). Lines are linear fit $\propto m * N/Z$. From figure, we see that E_{bal} decreases with increase in N/Z for all the systems. The decrease in E_{bal} is linear with $|m|$ 33, 25, 21, 18, and 15 for Ca+Ca, Ni+Ni, Zr+Zr, Sn+Sn and Xe+Xe series, respectively. Since we are having isotopes of elements so Coulomb potential will be same throughout the given isotopic series. Moreover, in recent study [22], Sood have shown that the effect of isospin dependence of cross section is same for the higher N/Z range for Ca+Ca series, thus does not affect the slope (m) of N/Z dependence of E_{bal} . This is expected for other systems as well. For a given series as the N/Z ratio increases, the neutron content also increases. Therefore, the repulsion due

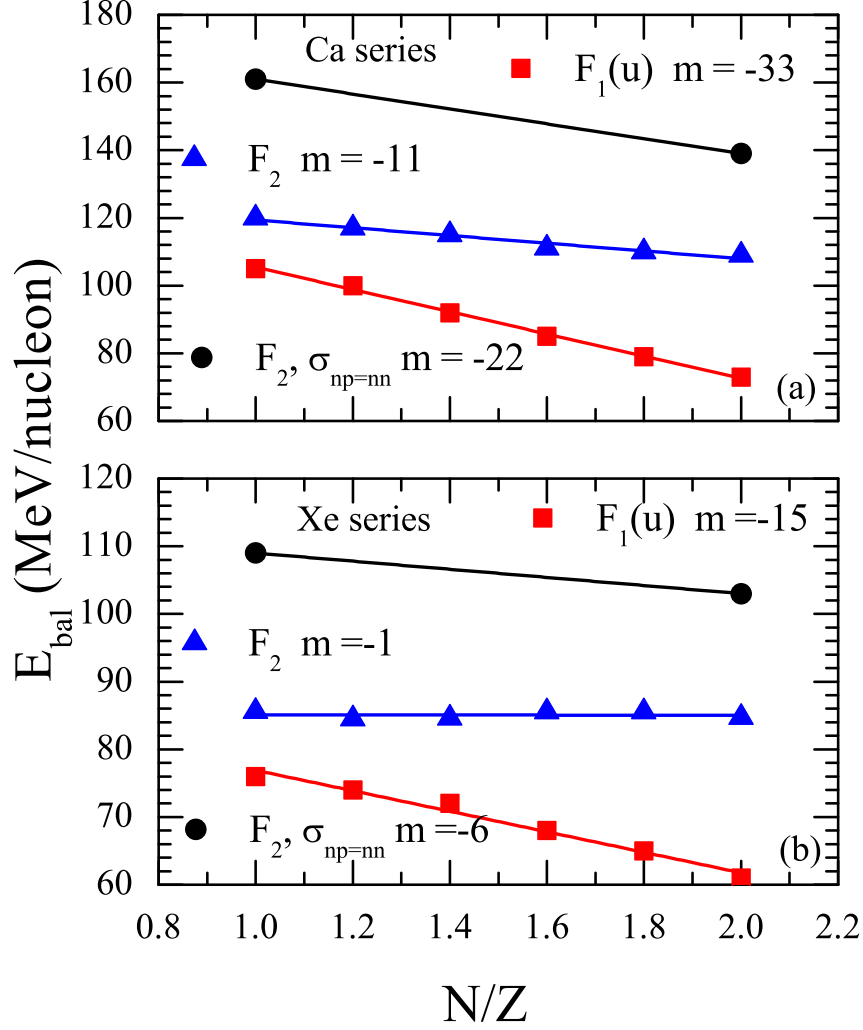


Figure 2: (Color online) N/Z dependence of E_{bal} for Ca+Ca and Xe+Xe with E_{sym} on and off. Various symbols are explained in text. Lines are linear fit.

to symmetry energy increases, hence the E_{bal} decreases with increase in N/Z .

To see the effect of symmetry energy on the N/Z dependence of E_{bal} throughout the mass range, we make the strength of potential part of symmetry energy zero (represented by F_2 , solid triangles) and calculate E_{bal} for two extreme mass systems Ca+Ca and Xe+Xe throughout the N/Z range. Results are displayed in Fig. 2(a) and Fig. 2(b), respectively, for Ca+Ca and Xe+Xe. Squares represent calculations with symmetry energy. We see

that when we reduce the strength of symmetry energy to zero, the slope of N/Z dependence of E_{bal} decreases drastically for both Ca and Xe series. This indicates that the effect of symmetry energy on the N/Z dependence of E_{bal} for a given isotopic series is of the same order throughout the mass range. Interestingly, we find that E_{bal} is same throughout the N/Z range for Xe series when we switch off the symmetry energy. Whereas for Ca series there is small decrease in E_{bal} with N/Z . To further explore this point we make the cross section isospin independent ($\sigma_{np} = \sigma_{nn}$) and calculate E_{bal} for two extreme $N/Z = 1.0$ and 2.0 for both Ca+Ca and Xe+Xe reactions. The results are displayed by circles. We see that the slope of N/Z dependence of E_{bal} increases when we switch off the symmetry energy and also take $\sigma_{np} = \sigma_{nn}$ as compared to when we switch off symmetry energy but cross section is isospin dependent. This is because E_{bal} decreases by large amount for $N/Z = 1.0$ for both Ca+Ca and Xe+Xe reactions which indicates larger role of isospin dependence of cross section for systems with $N/Z = 1.0$ as compared to for systems with $N/Z = 2.0$ (see Ref. [22] also) throughout the mass range. Therefore, the slope of N/Z dependence of E_{bal} decreases on inclusion of isospin dependence of cross section. From Fig. 2 we also see the role of symmetry energy in systems with $N/Z = 1$ (compare triangle and square at $N/Z = 1$) although symmetry energy contribution is not expected to be present in this case. To explore this, we calculate for $^{40}\text{Ca}+^{40}\text{Ca}$, the transverse flow of particles having $\rho/\rho_0 \leq 1$ (denoted as BIN 1) and particles having $\rho/\rho_0 > 1$ (denoted as BIN 2), respectively at all the time steps. The incident energy is taken to be 100 MeV/nucleon. The results are displayed in Fig. 3.

Solid (dashed) lines represent the $\langle p_x^{dir} \rangle$ of particles lying in BIN 1 (BIN 2). Dotted lines represent the total $\langle p_x^{dir} \rangle$. Upper (lower) panel is for calculations with (without) symmetry energy. We see that the total $\langle p_x^{dir} \rangle$ is sensitive to the symmetry energy even for symmetric systems like $^{40}\text{Ca}+^{40}\text{Ca}$ with $N/Z = 1$. This is because during the initial stages (between about 5-15 fm/c) the $\langle p_x^{dir} \rangle$ due to particles in BIN 1 is positive. The duration for which it remains positive is enhanced when we include the symmetry energy (compare shaded area in Fig. 3(a) and 3(b)). This is because in the spectator region (where high rapidity particles lie), the repulsive (attractive) symmetry energy for neutrons (protons) will accelerate the neutrons (protons) away (towards) the overlap zone. Inside the overlap zone the particles are stopped due to collisions. Since these particles belong to same midrapidity region, their momenta (due to symmetry potential) will add up to the zero thus nullifying the effect of symmetry potential for protons whereas the

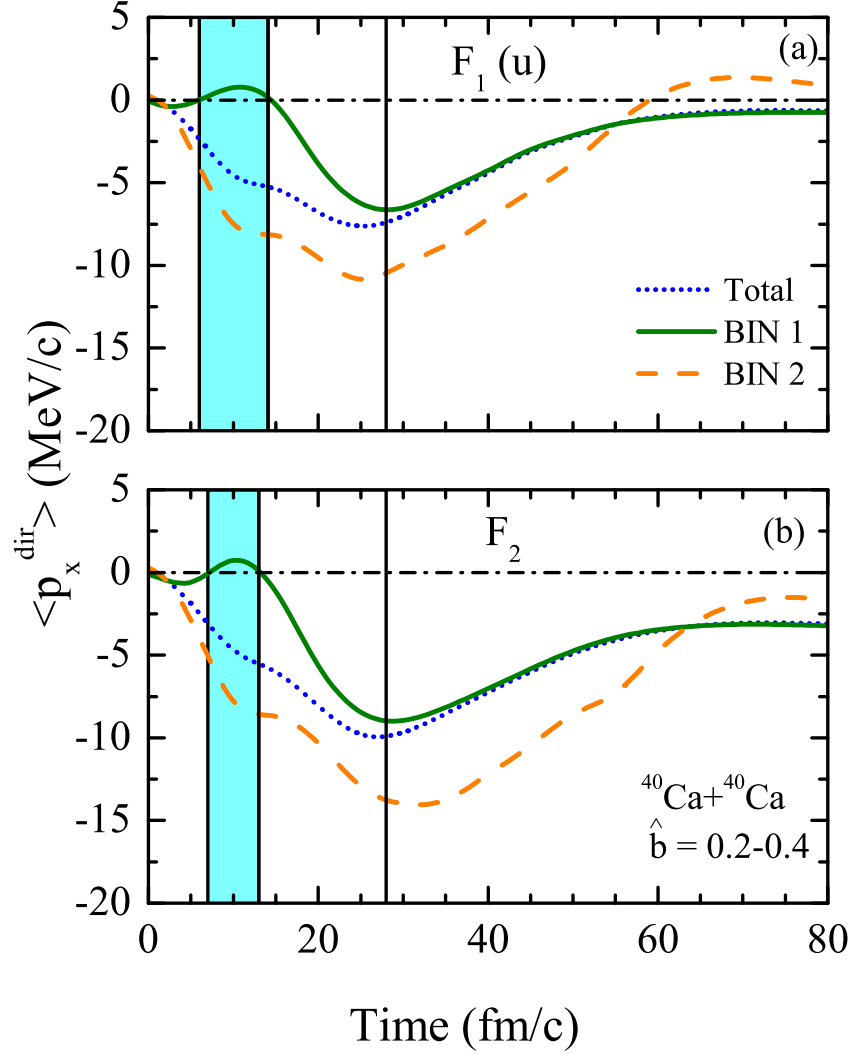


Figure 3: (Color online) The time evolution of $\langle p_x^{dir} \rangle$ for $^{40}\text{Ca}+^{40}\text{Ca}$ reaction for calculations with (upper panel) and without (lower) symmetry energy at 100 MeV/nucleon. Lines are explained in text.

neutrons will end up in spectator rapidity region leading to a net momentum due to the effect of symmetry energy. After about 15 fm/c, $\langle p_x^{dir} \rangle$ of particles lying in the BIN 1 becomes negative because these particles will now be attracted towards central dense zone. These particles will feel the attractive mean field potential up to about 25 fm/c after which the high density phase is over. The decrease in total $\langle p_x^{dir} \rangle$ due to attractive mean field potential (between 15-25 fm/c) is less when we include the symmetry potential in our calculations (compare the slopes of dotted curves (total $\langle p_x^{dir} \rangle$) in Fig. 3(a) and 3(b) between the right edge of shaded area and vertical line). This is because the

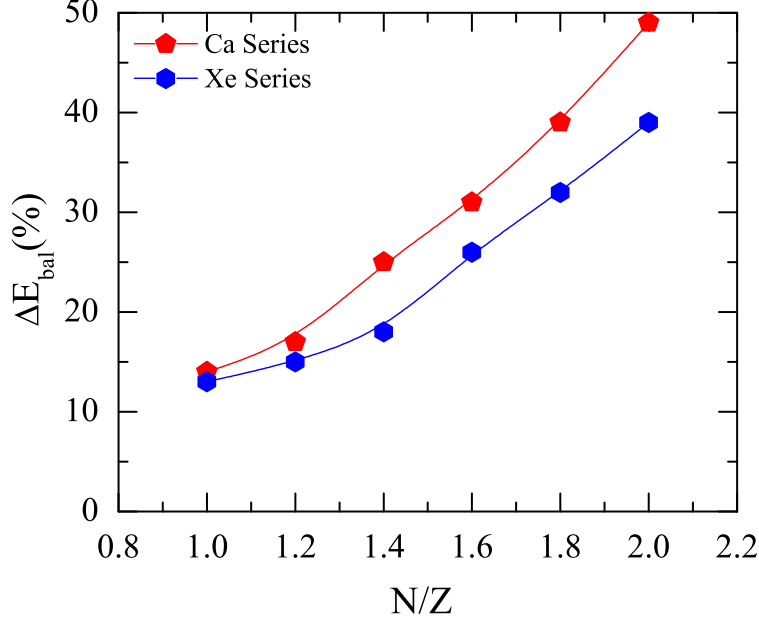


Figure 4: N/Z dependence of $\Delta E_{bal}(\%)$ for Ca and Xe series. Various symbols are explained in text. Lines are only to guide the eye.

neutrons due to the effect of symmetry energy lie in the spectator rapidity region with momenta away from the overlap zone. The attractive mean field potential will have to decelerate those particles first, make them stop and then accelerate the particles back towards the overlap zone. After about 30 fm/c, total $\langle p_x^{dir} \rangle$ follows the $\langle p_x^{dir} \rangle$ of particles lying in BIN 1 because of the expansion phase of the system. This explains the effect of symmetry energy in system with $N/Z = 1$. This effect is enhanced with increase in N/Z of the system [33].

In Fig. 4, we display the percentage difference ($\Delta E_{bal}(\%) = \frac{E_{bal}^{symmoff} - E_{bal}}{E_{bal}}$) between calculations without symmetry energy and with symmetry energy as a function of N/Z for Ca (pentagons) and Xe (hexagons) series. We see that the percentage difference increases with increases in N/Z for both Ca and Xe series, which shows that the effect of symmetry energy increases with increase in N/Z . The increase is more sharp for Ca series as compared to Xe, which indicates that with increase in N/Z the effect of symmetry energy increases more sharply for Ca as compared to Xe series. We also see that for $N/Z = 1.0$, the role of symmetry energy is same throughout the mass range as far as E_{bal} is

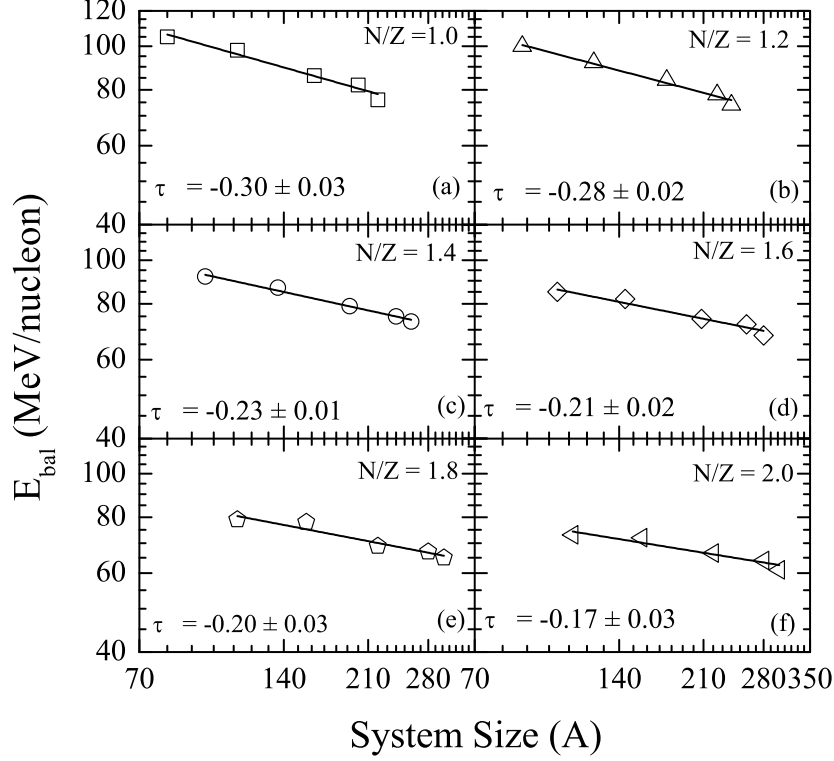


Figure 5: System size dependence of E_{bal} for various N/Z ratios. Lines are of power law fit ($\propto A^\tau$).

concerned. Thus, the N/Z dependence of E_{bal} for the isotopic series of lighter systems is a slightly better probe as compared to for heavier systems for constraining the symmetry energy.

In Fig. 5, we display the system size dependence of E_{bal} throughout the mass range. We find that for each N/Z , E_{bal} follows a power law behavior ($\propto A^\tau$) with power law parameter $\tau = -0.30 \pm 0.03$, -0.28 ± 0.02 , -0.27 ± 0.01 , -0.21 ± 0.02 , and -0.20 ± 0.03 for $N/Z = 1.0$ (open squares), 1.2 (triangles), 1.4 (circles), 1.6 (diamonds), 1.8 (open pentagons), and 2.0 (left triangles), respectively. We find that the value of τ decreases with increase in N/Z of the systems. This is due to that fact that for higher N/Z ratio the effect of symmetry energy is more in lighter masses (as discussed previously), thus decreasing the E_{bal} by larger magnitude on inclusion symmetry energy in lighter masses which results in less slope for higher N/Z ratio. Here we would like to stress that with increase in N/Z

for a given mass (compare mass of about 120 in Fig. 5(a) and 5(b)), the E_{bal} decreases which is quite the opposite trend to the data [26]. Since we have taken the isotopes of a given element, so that the Coulomb is same for a given series. This is because we have shown clearly in Ref. [20, 21] that Coulomb repulsion plays much more dominant role over symmetry energy in isospin effects (if one considers isobars) throughout the mass range and colliding geometry.

4 Summary

We have studied the N/Z dependence of balance energy (E_{bal}) for isotopic series throughout the mass range. We found drastic effect of symmetry energy on the N/Z dependence of E_{bal} throughout the mass range. We also found that the N/Z dependence of E_{bal} for isotopic series of lighter system is slightly more sensitive to symmetry energy as compared to that of heavier systems. We have also studied the mass dependence of E_{bal} for the N/Z range from 1.0-2.0. We found that the mass dependence of E_{bal} varies with the N/Z ratio.

This work is supported by a grant from Centre of Scientific and Industrial Research (CSIR), Government of India and Indo-French center vide project no-4101-A, New Delhi, India.

References

- [1] R. K. Puri et al, J. Phys. G: Nucl. Part. Phys. **18**, 903 (1992); *ibid*, G18, 1533 (1992); *ibid.*, Phys. Rev. C **45**, 1837 (1992); *ibid*, C43, 315 (1991) *ibid.*, Eur. Phys. J. A **3**, 277 (1998); *ibid.* **A23**, 429 (2005); S. S. Malik et al, Pramana J. Phys. **32**, 419 (1989); R. Arora *et al.*, Eur. Phys. J A **8**, 103 (2008); I. Dutt *et al.*, Phys. Rev. C **81**, 064608 (2010); *ibid.* **81**, 064609 (2010); *ibid.* **81**, 047601 (2010); *ibid.* **81**, 044615 (2010).
- [2] S.W. Huang *et al.*, Phys Letts. B **41**, 298 (1993); *ibid.* Prog. Nucl. Part Phys. **30**, 105 (1993).
- [3] C. L. Jiang, B. B. Back, H. Esbensen, R. V. F. Janssens, and K. E. Rehm, Phys. Rev. C **73**, 014613 (2006); N. G. Nicolis, Eur. Phys. J. A **21**, 265 (2004).

- [4] C. Sturm *et al.*, Phys. Rev. Lett. **86**, 39 (2001); C. Hartnack, J. Jaenicke, L. Shen, H. Stöcker, and J. Aichelin, Nucl. Phys. **A580**, 643 (1994).
- [5] J. Singh *et al.*, Phys. Rev. C **65**, 024602 (2002); S. Kumar *et al.*, *ibid.* **78**, 064602 (2008); D. Sisan *et al.*, *ibid.* **63**, 027602 (2001).
- [6] A. D. Sood and R. K. Puri, Phys. Rev C **70**, 034611 (2004); R. Chugh *et al.*, *ibid.* **82**, 014603 (2010).
- [7] A. D. Sood and R. K. Puri, Phys. Rev. C **73**, 067602 (2006); D. J. Magestro *et al.*, Phys. Rev. C **61**, 021602(R) (2000); D. J. Magestro *et al.*, Phys. Rev. C **62**, 041603(R) (2000); G. D. Westfall *et al.*, Nucl. Phys. A **681**, 342c (2001).
- [8] B. A. Li, Phys. Rep. **464**, 113 (2008).
- [9] A. D. Sood and R. K. Puri, Phys. Lett. **B594**, 260 (2004); S. Kumar et al, Phys Rev. C **58**, 3494 (1998).
- [10] A. D. Sood and R. K. Puri, Eur. Phys. J. A **30**, 571 (2006).
- [11] A. D. Sood and R. K. Puri, Phys. Rev. C **69**, 054612 (2004); *ibid* , C79, 064618 (2009).
- [12] C. A. Ogilvie *et al.*, Phys. Rev. C **40**, 2592 (1989); B. Blättel, V. Koch, A. Lang, K. Weber, W. Cassing, and U. Mosel, *ibid.* **43**, 2728 (1991).
- [13] Q. Pan and P. Danielewicz, Phys. Rev. Lett. **70**, 2062 (1993); J. Lukasik *et al.*, Phys. Lett. **B608**, 223 (2005); V. Ramillien *et al.*, Nucl. Phys. **A587**, 802 (1995).
- [14] Y. Zhang and Z. Li, Phys. Rev. C **74**, 014602 (2006); B. Hong *et al.*, Phys. Rev. C **66**, 034901 (2000); L. Scalone, M. Colonna, and M. Di Toro, Phys. Lett. **B461**, 9 (1999).
- [15] D. Krofcheck *et al.*, Phys. Rev. Lett. **63**, 2028 (1989).
- [16] W. Zhan *et al.*, Int. J. Mod. Phys. E **15**, 1941 (2006); see, e.g. <http://www.impcas.ac.cn/zhuye/en/htm/247.htm>.
- [17] See, e.g., http://www.gsi.de/fair/index_e.html; See, e.g., <http://ganiinfo.in2p3.fr.research/developments/spiral2>.

- [18] Y. Yano, Nucl. Inst. Methods B **261**, 1009 (2007).
- [19] B. A. Li, Z. Ren, C. M. Ko, and S. J. Yennello, Phys. Rev. Lett. **76**, 4492 (1996);
C. Liewen, Z. Fengshou, and J. Genming, Phys. Rev. C **58**, 2283 (1998).
- [20] S. Gautam and A. D. Sood, Phys. Rev. C **82**, 014604 (2010).
- [21] S. Gautam *et al.*, Phys. Rev. C **83**, 014603 (2011); *ibid.*, J. Phys G:Nucl. Part. Phys. **37**, 085102 (2010).
- [22] A. D. Sood, Phys. Rev. C. (communicated), *nucl-th*/1012.5873.
- [23] C. Hartnack *et al.*, Eur. Phys. J. A **1**, 151 (1998); C. Hartnack and J. Aichelin, Phys. Rev. C **49**, 2801 (1994); S. Kumar *et al.*, *ibid.* **81**, 014611 (2010); *ibid.* **81**, 014601 (2010).
- [24] J. Aichelin, Phys. Rep. **202**, 233 (1991); D. T. Khoa *et al.*, Nucl. Phys. **A548**, 102 (1992); Y. K. Vermani *et al.*, J. Phys. G: Nucl. Part. Phys. **36**, 105103 (2009); *ibid.* **37**, 115105 (2010); *ibid.* Eur Phys Lett **85**, 62001 (2010); *ibid.* Phys. Rev. C **79**, 064613 (2009), Nucl. Phys A **847**, 243 (2010);
- [25] E. Lehmann *et al.*, Phys. Rev. C **51**, 2113 (1995); *ibid*, Prog. Nucl. Part Phys., 30, 219 (1993); G. Batko *et al.*, *ibid.* **20**, 461 (1994); R. K. Puri *et al.*, Nucl. Phys. A **575**, 733 (1994); J. Singh *et al.*, Phys. Rev. C **67**, 044617 (2000); R.K. Puri and J. Aichelin, J. Comp Phys. **162**, 245 (2000); S. Kumar *et. al.*, Phys Rev. C **58**, 320 (1998); *ibid.*, **57**, 2744 (1998); J. Dhawan *et al.*, *ibid.*, **74**, 057901 (2006).
- [26] R. Pak R *et al.*, Phys. Rev. Lett **78**, 1022 (1997); *ibid.* **78**, 1026)1997).
- [27] J. Cugnon, T. Mizutani, and J. Vandermeulen, Nucl. Phys. **A352**, 505 (1981).
- [28] E. Lehmann *et al.*, Z. Phys. A **355**, 55 (1996).
- [29] G. D. Westfall *et al.*, Phys. Rev. Lett. **71**, 1986 (1993).
- [30] G. D. Westfall, Nucl. Phys. **A630**, 27c (1998).
- [31] D. Cussol *et al.*, Phys. Rev. C **65**, 044604 (2002).

- [32] C. A. Ogilvie *et al.*, Phys. Rev. C **40**, 2592 (1989).
- [33] S. Gautam *et al.*, Phys. Rev. C **83**, 034606 (2011).